Pretreatment of kaempferol-3-O-rutinoside protects H9c2 cells against LPS-induced inflammation through the AMPK/SIRT1 pathway

Yao-yao Ma[1], Xiao-ni Zhao[1], Lan Zhou[1], Sheng-nan Li[2], Juan Bai[2], Ling-li Shi[2], Fang Hua[2]*, Peng Zhou[1]*

[1]Department of Integrated Traditional Chinese and Western Medicine, Anhui University of Chinese Medicine, Anhui, P.R. China; [2]School of Pharmacy, Anhui Xinhua University, Anhui, P.R. China

***Corresponding Authors:** Fang Hua, School of Pharmacy, Anhui Xinhua University, Anhui, P.R. China. Email: happyhf6941@sina.com; Peng Zhou, Department of Integrated Traditional Chinese and Western Medicine, Anhui University of Chinese Medicine, Anhui, P.R. China. Email: zhoupeng@ahtcm.edu.cn

Received: 14 October 2022; Accepted: 17 February 2023; Published: 17 April 2023

OPEN ACCESS

ORIGINAL ARTICLE

Abstract

Kaempferol-3-O-rutinoside (KR) is a flavonoid glycoside derived from traditional Chinese medicine, plants, and tea, and has good myocardial protection. This study focuses on the mechanism of myocardial protection with KR and whether myocardial protection can be achieved by activating the adenosine monophosphate-activated protein kinase–silent mating-type information regulation 2 homolog 1 (sirtuin) (AMPK/SIRT1) signal pathway. Molecular docking technique was used to predict the binding affinity of KR to AMPK. The inflammatory injury model of H9c2 cells was established by lipopolysaccharide (LPS) induction. H9c2 cell proliferation was detected by cell counting kit-8 assay. The apoptosis rate was measured by flow cytometry. Levels of interlukin (IL)-1β, IL-6, and tumor necrosis factor-α (TNF-α) were determined by enzyme-linked-immunosorbent serologic assay. AMPK and SIRT1 expression levels were quantified through reverse transcription-polymerase chain reaction and Western blotting assay. Results indicated that KR has a certain binding affinity with AMPK. KR could increase the growth of H9c2 inhibited by LPS, reduce apoptosis rate, and reverse the elevated levels of IL-1β, IL-6, and TNF-α. Furthermore, KR could suppress the expression levels of AMPK and SIRT1, and AMPK-specific inhibitor (Compound C) could significantly counteract the activation of KR, indicating that its anti-inflammatory effect is achieved by regulating the AMPK/SIRT1 signaling pathway.

Keywords: AMPK/SIRT1 signaling pathway, inflammation, kaempferol-3-O-rutinoside, myocardial protection

Introduction

At present, the incidence of cardiovascular diseases (CVD) and accounted mortality are on the rise in China. CVD mortality ranks first among all causes, accounting for more than 40% of the disease deaths in China (Zhao *et al.*, 2019). Chronic heart failure (CHF) is a common cardiovascular disease and a serious end-stage of various heart diseases, which seriously threatens the health of patients (D'Alessandra *et al.*, 2020). Ventricular remodeling (VR) after acute myocardial infarction (AMI) is the pathophysiological basis for the development of CHF (Zhao *et al.*, 2021). The myocardium in the infarcted area becomes thinner and dilated, while the myocardium in the non-infarcted area becomes hypertrophic and elongated, leading to the enlargement and deformation of the ventricular cavity, resulting in decrease of ventricular systolic function (Schumacher *et al.*, 2019). The resulting VR extends through the whole course of the disease and is an important risk factor for long-term death. Therefore, to explore how to prevent or reverse VR after AMI and delay or inhibit the pathophysiological process of AMI after CHF is an inevitable choice to effectively improve the prognosis of AMI patients and prevent and treat CHF.

Adenosine monophosphate-activated protein kinase (AMPK) is an evolutionarily conserved serine/threonine protein kinase, known as the "cellular energy regulator." It plays an important role in maintaining cell and energy balance (Herzig and Shaw, 2018). AMPK exists in the form of α, β, and γ, and is directly activated by interaction between Sestrin1 and Thr 172, which have been demonstrated in cardiomyocytes (Yuan *et al.*, 2022). When activated, AMPK maintains cell energy balance, turning on the productive catabolic pathway while shutting down the energy-consuming synthetic pathway, which contributes to cell survival and cardiovascular system function when cells are hypoxic (Wu and Zou, 2020; Zhao *et al.*, 2022). Studies have shown that normal energy metabolism of the myocardium is the material basis for maintaining the stability of cardiac internal environment and myocardial systolic function. After myocardial ischemia, the substrate of myocardial tissue energy supply is transformed from fatty acid β oxidation to anaerobic glycolysis of glucose, leading to the accumulation of free fatty acid (FFA) and lactic acid and insufficient myocardial energy supply (Wang *et al.*, 2019). Therefore, it is possible to improve the activity of AMPK and promote its anti-inflammatory effect to achieve anti-VR after AMI.

Kaempferol-3-O-rutinoside (KR) is a flavonoid glycoside extracted from traditional Chinese medicine, plants, and tea. A previous study has found that Lu´an GuaPian tea has the highest content of KR (Bai *et al.*, 2017). Evidence has found that KR is beneficial for human health, including anti-diabetic activity, and cerebral protective, hepatoprotective, anti-cancer, and cardioprotective effects (Hua *et al.*, 2018; Li *et al.*, 2021; Wang *et al.*, 2015, 2021; Yu *et al.*, 2021). The outstanding effect of KR is that it has a good protective effect on myocardial cells. Previous studies have found that KR improves hemodynamics and cardiac function, reduces myocardial fibrosis and cardiomyocyte apoptosis, and decreases excessive release of inflammatory factors by inhibiting nuclear factor kappa B–oligomerization domain-like receptor family pyrin domain-containing 3–caspase-1 (NF-κB/NLRP3/Caspase-1) signaling pathway. The myocardial protective effect of KR is related to its regulation of NF-κB/NLRP3/Caspase-1 signaling pathway (Hua *et al.*, 2022). However, the activation of NF-κB is regulated by the upstream AMPK–silent mating type information regulation 2 homolog 1 (sirtuin) (SIRT1) signaling pathway, which leads to myocardial cell damage (Chen *et al.*, 2018). It is speculated that KR may be one of the important pathways to prevent and treat myocardial cell injury by regulating the inflammatory response of AMPK/SIRT1 signal pathway.

In this study, molecular docking was used to predict the target AMPK of KR. It was verified by *in vitro* experiments, which were used to explore the role of KR *in vitro* underlying molecular mechanisms.

Materials and Methods

Chemicals and materials

The purity of KR is more than 98% (Desite Biotechnology Co. Ltd., Chengdu, China). AMPK-specific inhibitor (Compound C) was obtained from Abmole Bioscience Inc. (USA). Lipopolysaccharide (LPS, Cat. No. L8880) was obtained from Solarbio Science & Technology Co. Ltd. (Beijing, China). Fetal bovine serum (FBS, BL201A) and Dulbecco's modified eagle medium (DMEM, BL304A) were purchased from Biosharp (China). Penicillin–streptomycin solution was purchased from Shandong SparkJade Biotechnology Co. Ltd. (China). Mouse tumor necrosis factor-α (TNF-α; MM-0180R1), interlukin (IL)-1β (MM-0047R1), IL-6 (MM-0190R1) and enzyme-linked-immunosorbent serologic assay (ELISA) kits were bought from Meimian (Jiangsu, China). Anti-p-AMPKα (AF3423) and anti-SIRT1 (DF6033) were purchased from Affinity Biosciences (Melbourne, Australia). Anti-glyceraldehyde 3-phosphate dehydrogenase (GAPDH, 380626) was purchased from ZEN-Bio Science (Chengdu, China). Trizol (G3013), SYBR (G3326), and Annexin V-FITC/PI cell apoptosis detection kit (G1511) were purchased from Servicevbio Biotechnology Co. Ltd. (Wuhan, China).

Molecular docking

The CB-Dock molecular docking platform was used to calculate center and size of the target cavity, and ligand was uploaded for molecular docking. Protein data bank (PDB) formats of AMPK (PDB code: 4CFF) (Xiao *et al.*, 2013) and KR or A-769662 in Spatial Data File (SDF) format were input to CB-Dock for molecular docking (Liu *et al.*, 2020).

In vitro experiment

Cell culture and treatment

DMEM containing 10% FBS, 1% penicillin–streptomycin in DMEM were used to culture H9c2 cells at 37°C and 5% CO_2. H9c2 cells in logarithmic growth phase were trypsinized with 0.25% and seeded in six-well plates. For pharmacodynamic study, H9c2 cells were divided into the following three groups: control group, model group (10-μg·ml^{-1} LPS), and KR group (25-μM KR). H9c2 cells were pre-incubated with KR for 12 h. Then, H9c2 cells were stimulated with 10-μg·ml^{-1} LPS for 6 h (Fanghua). To further investigate the effect of KR on AMPK, H9c2 cells were divided into the following five groups: control group, model group, KR group, Compound C group (10-μM Compound C), and KR+Compound C group (25-μM KR + 10-μM Compound C). H9c2 cells were

pre-incubated with KR, Compound C, or KR+Compound C for 12 h, and stimulated with LPS for 6 h.

Detection of H9c2 cells proliferation by cell counting kit-8 (CCK-8) assay

H9c2 cells were seeded into 96-well plates at a density of 3×10^3 cells/well. The cells were incubated with 10% CCK-8 (SparkJade, 10 μL) solution at 37°C for 1 h. After mixing, optical density (OD) at 450 nm was measured with LabServ K3 microplate reader.

Detection of apoptosis by flow cytometry

Cell culture supernatants were collected, digested with ethylenediaminetetraacetic acid (EDTA)-free trypsin, and centrifuged. After obtaining H9c2 cells, washed twice with phosphate-buffered saline (PBS) solution, and harvested and dissociated into single-cell suspensions. A 100-μL cell suspension was added with 5-μL Annexin V-FITC and 5-μL propidium iodide (PI), mixed and incubated for 10 min at room temperature in the dark (Tang *et al.*, 2022). Then, 400-μL staining buffer was added prior to detection by Beckman DxFlex flow cytometer (Beckman, USA) and analyzed using FlowJo V10.

Detection of IL-1β, IL-6, and TNF-α by ELISA

H9c2 cells were seeded in a 6-well plate (5×10^4 cells/well) and incubated at 37°C and 5% CO_2. With appropriate intervention, the supernatant was collected by centrifugation at 1,000 g for 10 min. IL-1β, IL-6, and TNF-α were detected by ELISA.

Detection of protein expression by Western Blotting assay

The bicinchoninic acid assay (BCA) kit was used to determine the concentration of protein. Proteins were separated by sodium dodecyl sulfate–polyacrylamide gel electrophoresis (SDS-PAGE). After lysis of H9c2 cells in lysate, the supernatant was removed after centrifugation, 4X loading buffer was added, and the protein was fully denatured through boiling. The proteins were separated on 10% polyacrylamide gel and transferred to a polyvinylidene fluoride (PVDF) membrane; then blocked in 5% skimmed milk powder for 2 h and incubated overnight at 4°C. Specific proteins were identified using antibodies against p-AMPK (1:1,000), SIRT1 (1:500), and GAPDH (1:5,000). The membranes were incubated for 2 h the next day with horseradish peroxidase (HRP)-conjugated secondary antibodies corresponding to primary antibody. Electrogenerated chemiluminescence (ECL) (Biosharp, BL520B) was used to develop and fix, and gel imager (Tanon 5200 Imaging System, China). The experiment was repeated thrice. Image J was used to analyze gray values of the bands.

Detection of messenger RNA (mRNA) expression by reverse transcription-polymerase chain reaction (RT-PCR)

After KR treatment, defrost template RNA and reagent on ice, mix, and centrifuge the solution. Preparation of reaction system on ice in RNase free tube: The dose of RNA was determined by using Eppendorf BioPhotometer plus (OD 1.8–2.0), μL 5*Reaction Mix, 3-μL supreme enzyme mix, and diethyl pyrocarbonate (DEPC)-treated water was replenished to 20 μL. After mixing, the program was run as follows: at 25°C for 10 min, random primers were paired with RNA templates to remove genomic DNA, and at 55°C for 15 min, reverse transcription reaction and double-stranded DNA (dsDNase) were rapidly inactivated. Reverse transcriptase was inactivated at 85°C for 5 min, and the final complementary DNA (cDNA) product was obtained. RT-PCR was performed using the SYBR Green PCR Kit. All PCR reactions were performed up to 10-μL volume using the Roche LightCycler 96. The amplification procedure includes the following: pre-denaturing at 95°C for 5 min, then denaturing at 95°C for 15 s, annealing at 60°C for 60 s, and performing PCR under 40 cycles. The melting curve is from 60°C to 95°C. mRNA expression levels of AMPK and SIRT1 were analyzed using $2^{-\Delta\Delta Cq}$ method, and were normalized to GAPDH. The primer sequences used are shown in Table 1.

Results

Molecular docking results

Molecular docking results showed that KR had a certain binding activity with AMPK (Table 2 and Figure 1). Vina score of KR was significantly higher than its ligand (SBI-0206965). The docking results were further verified by *in vitro* experiments.

KR promoted H9c2 cells proliferation under LPS treatment

H9c2 cells were cultured with KR at 25 μM for 12 h. CCK8 assay confirmed that KR significantly increased LPS-induced H9c2 cell survival ($p < 0.01$). KR appreciably increased the growth of H9c2 inhibited by LPS (Figure 2).

Table 1. Primers used in RT-qPCR.

Primers	Sequence (5′ → 3′)	
AMPK	Forward	5′-GCCGAGAAGCAGAAGCACGAC-3′
	Reverse	5′-GCTTGCCCACCTTCACTTTCCC-3′
SIRT1	Forward	5′-AGTAACAGTGACAGTGGCACATGC-3′
	Reverse	5′-CCTCCGTCAGCTCCAGATCCTC-3′
GAPDH	Forward	5′-AAGAGGGATGCTGCCCTTAC-3′
	Reverse	5′-ATCCGTTCACACCGACCTTC-3′

Table 2. Docking results of SBI-0206965 and KR with AMPK.

Compound	Vina score	Cavity score	Center (x, y, and z)	Size (x, y, and z)
SBI-0206965	–7.0	459	49, –43, 34	23, 23, 23
KR	–8.5	459	49, –43, 34	26, 26, 26

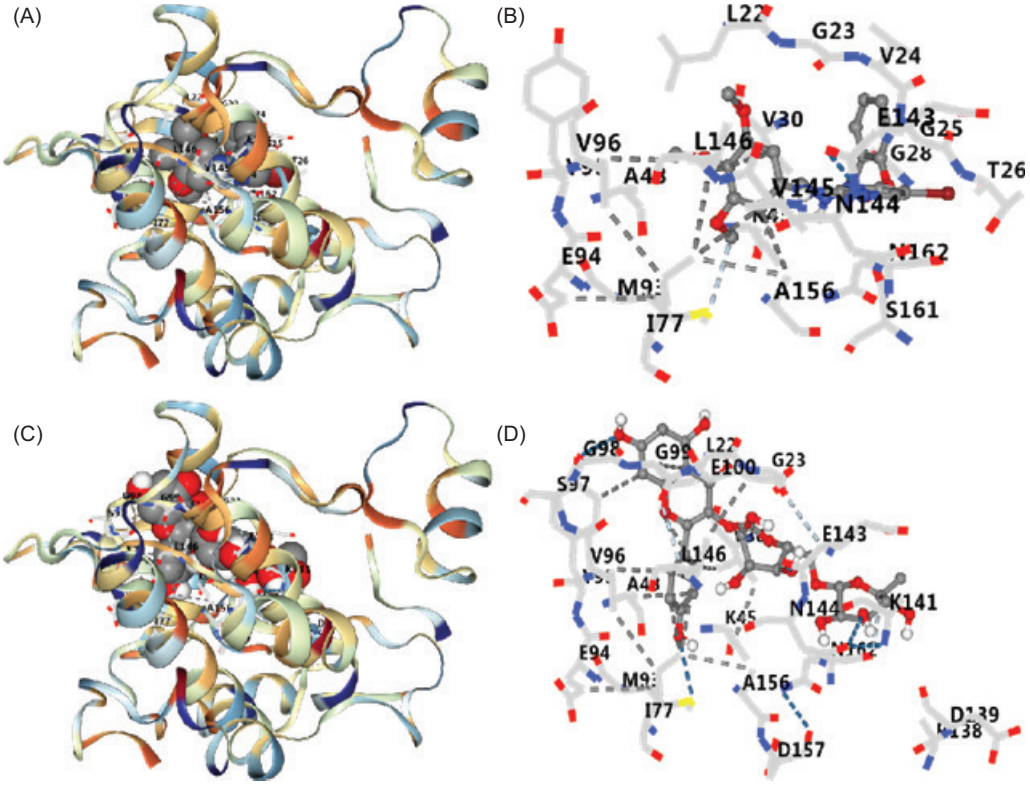

Figure 1. Docking results of SBI-0206965 and KR with AMPK. (A) 3D complex of SBI-0206965–AMPK. (B) Amino acid binding of SBI-0206965–AMPK. (C) 3D complex of KR-AMPK. (D) Amino acid binding of KR to AMPK. KR: kaempferol-3-O-rutinoside.

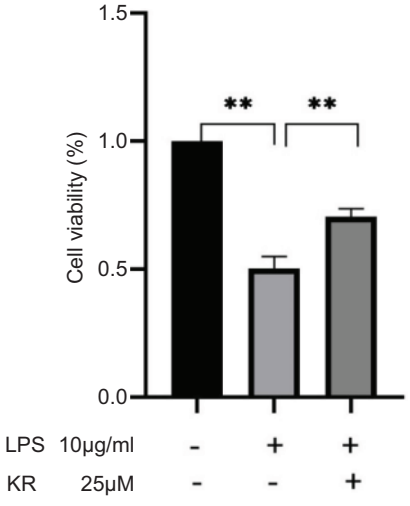

Figure 2. Kaempferol-3-O-rutinoside resists the proliferation of H9c2 cells inhibited by LPS. The values are expressed as mean ± SD (n = 3). **$p < 0.01$ vs the model group.

KR reduced the apoptosis rate of H9c2 cells induced by LPS

Compared to the control group, the apoptosis rate was significantly higher in the model group ($p < 0.001$). In contrast, KR can significantly reduce the apoptosis rate ($p < 0.001$) (Figure 3).

KR reduced the overexpression of inflammatory cytokines

Levels of IL-1β, IL-6, and TNF-α were increased significantly in the model group, compared to the control group ($p < 0.05$ and <0.01). KR could reverse the elevated levels of IL-1β, IL-6, and TNF-α ($p < 0.05$ and <0.01) (Figure 4). KR could inhibit the overexpression of inflammatory cytokines.

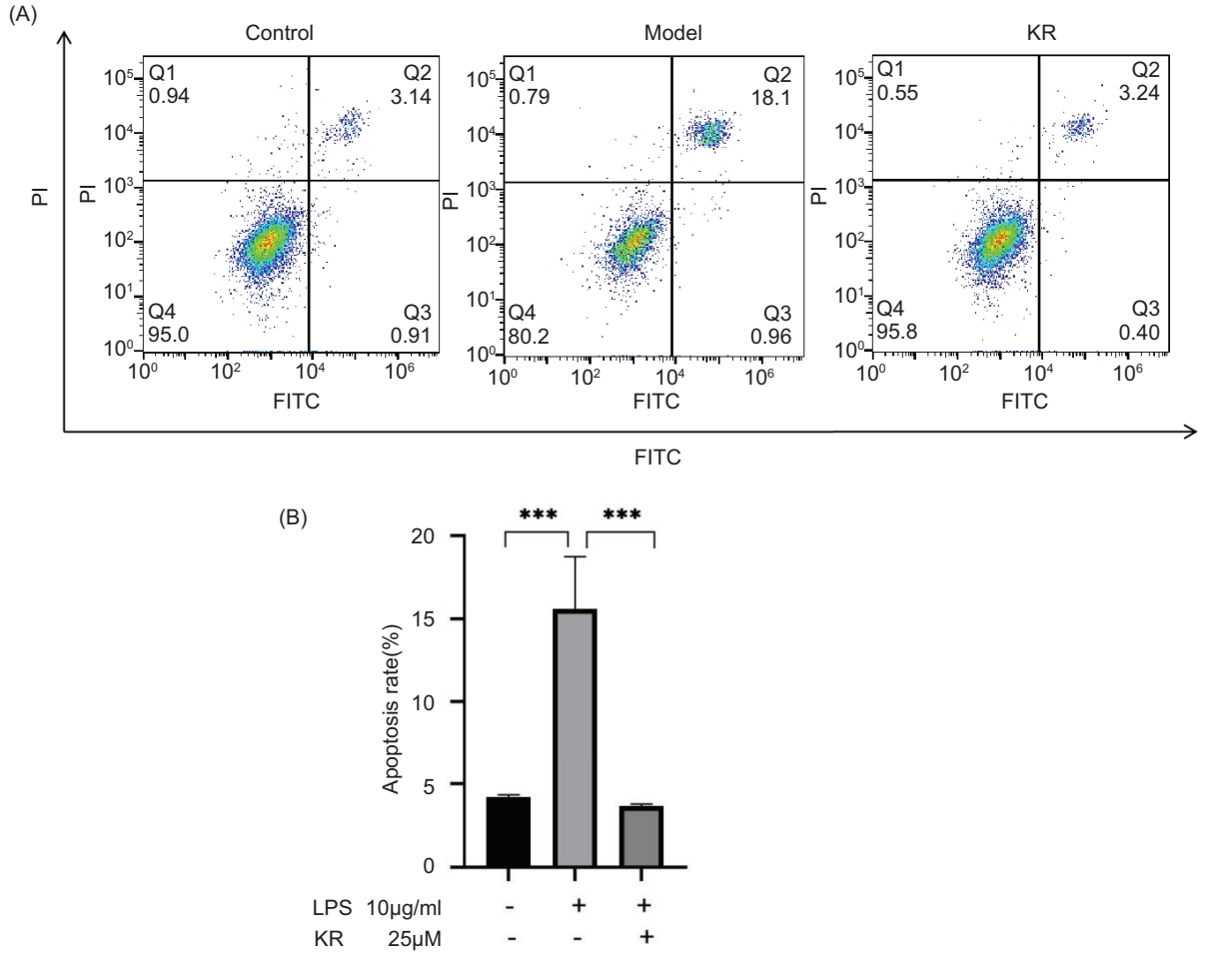

Figure 3. Kaempferol-3-O-rutinoside reduces the apoptosis rate of H9c2 cells induced by LPS. (A) The apoptosis rate is measured by flow cytometry. (B) Statistical chart of apoptosis rate. The values are expressed as mean ± SD (n = 3). ***$p < 0.001$ vs the model group.

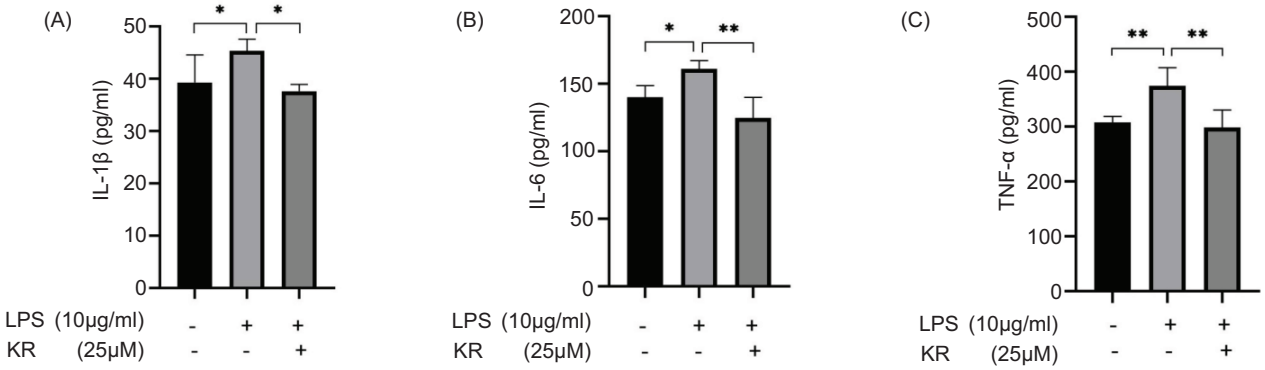

Figure 4. Kaempferol-3-O-rutinoside reduced the overexpression of inflammatory cytokines. (A) IL-1β, (B) IL-6, and (C) TNF-α. The values are expressed as mean ± SD (n = 6). *$p < 0.05$, **$p < 0.01$ vs the model group.

KR increased the mRNA expression levels of AMPK and SIRT1

Compared to the control group, the mRNA expression levels of AMPK and SIRT1 decreased considerably in the model group ($p < 0.01$). Compared to the model group, KR was able to reverse mRNA overexpression ($p < 0.01$) (Figure 5). The results pointed out that the protective effect of KR on LPS-induced myocardial cell damage was related to the activation of AMPK/SIRT1 signaling

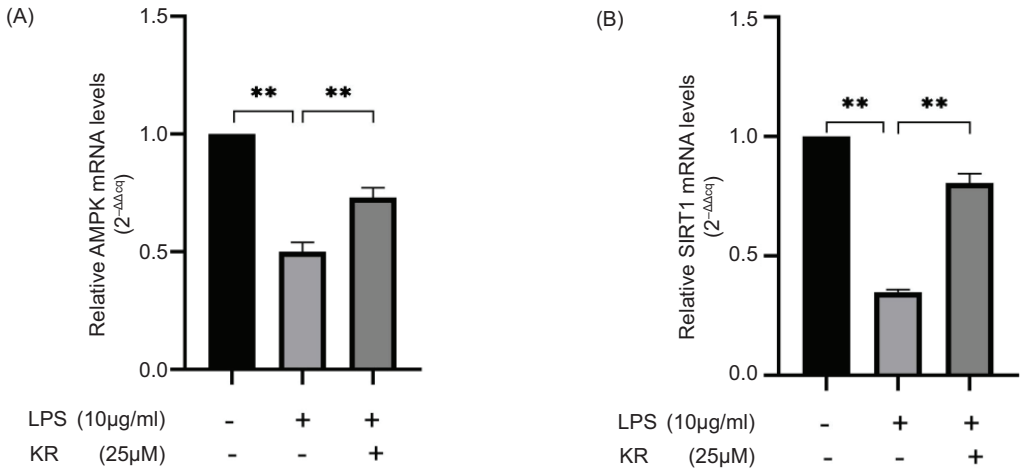

Figure 5. Kaempferol-3-O-rutinoside increased the mRNA expression levels of (A) AMPK and (B) SIRT1. The values are expressed as mean ± SD (n = 3). **p < 0.01 vs the model group.

pathway. Next, the mechanism was verified by using AMPK-specific inhibitors.

Effects of KR and Compound C on the protein expression level of AMPK/SIRT1 signal pathway

Protein expression levels of AMPK and SIRT1 in the model group decreased considerably, compared to the control group (p < 0.05 and <0.01). After treatment with KR, the expression levels of p-AMPK and SIRT1 was augmented (p < 0.05 and <0.01). After the intervention of Compound C, the expression levels of AMPK and SIRT1 were returned to the original level. After the combined application of KR and Compound C, Compound C could significantly counteract the activation of KR (p < 0.05) (Figure 6). Therefore, KR could play a role in myocardial protection by activating the AMPK/SIRT1 signal pathway.

Effects of KR and Compound C on the mRNA expression level of AMPK/SIRT1 signal pathway

The mRNA expression levels of AMPK and SIRT1 in the model group was consistent with the protein expression. After KR treatment, the mRNA expression levels of p-AMPK and SIRT1 were increased (p < 0.01). After combined application of KR and Compound C, the effect of Compound C on mRNA expression was consistent with those of protein, both of which have the effect of resisting KR (p < 0.01) (Figure 7).

Discussion

An acute inflammatory response occurs in the short term after AMI, and inflammatory cytokines, including IL-1β, IL-6, and TNF-α (Sun *et al.*, 2021). Inflammatory response plays an important role in the occurrence and development of VR. Therefore, it is very important to treat the over release of inflammatory factors against VR after AMI.

AMPK system is a novel anti-inflammatory signaling pathway, connecting with SIRT1 (sirtuin), *p53*, *FoxO3α*, and *p300* to control the occurrence and development of inflammation (Chen *et al.*, 2022). Therefore, AMPK activity can be improved to promote its anti-inflammatory effect and achieve the purpose of anti-VR after AMI. SIRT1 is a class of highly conserved protein deacetylases that catalyzes the deacetylation of histone and non-histone lysine residues, and is associated with important life activities, such as cell survival, proliferation, aging, apoptosis, cell metabolism, and energy restriction (Wu, 2021). SIRT1 exists in the nucleus and cytoplasm and plays an anti-inflammatory role, which is considered a potential therapeutic target for CVD (Chen *et al.*, 2020). AMPK promotes the transcription and activity of nicotinamide (NAM) phosphoribosyltransferase (Nampt) synthesized by nicotinamide adenine dinucleotide+ (NAD^+), increases the level of [NAD^+]/[NADPH], and mediates the activation of SIRT1, thus playing an anti-inflammatory function (Hurley *et al.*, 2021). SIRT1 then interacts with the RelA/p65 subunit of the NF-κB complex, which could deacetylate NF-κB p65 subunit Lys310 to inhibit NF-κB transcriptional activity (Deng *et al.*, 2021). In short, the anti-inflammatory mechanism of VR after AMI is closely related to the AMPK/SIRT1/NF-κB signaling pathway, that is, activation of AMPK may up-regulate SIRT1 expression, inhibit the activity of NF-κB inflammatory proteins, and down-regulate the expression of downstream inflammatory factors, thereby inhibiting the inflammatory response.

Kaempferol-3-O-rutinoside has a good cardiovascular protective effect, so it is important to further study

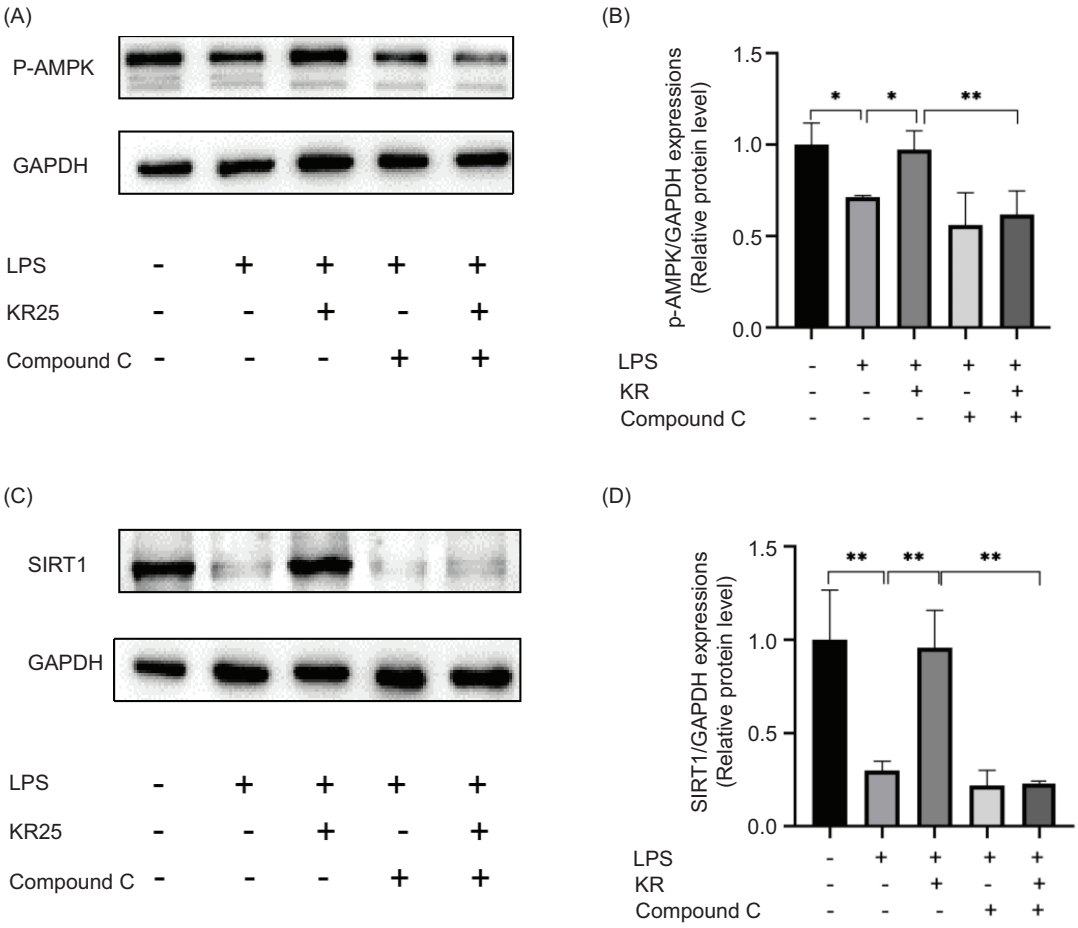

Figure 6. Effects of kaempferol-3-O-rutinoside (KR) and Compound C on the proteins of AMPK/SIRT1 signal pathway. (A) Picture of Western spots of p-AMPK, (B) p-AMPK. (C) Picture of Western spots of SIRT1, (D) SIRT1. The values are expressed as mean ± SD (n = 3), **p < 0.01, *p < 0.05 vs the model group; **p < 0.01 vs the KR group.

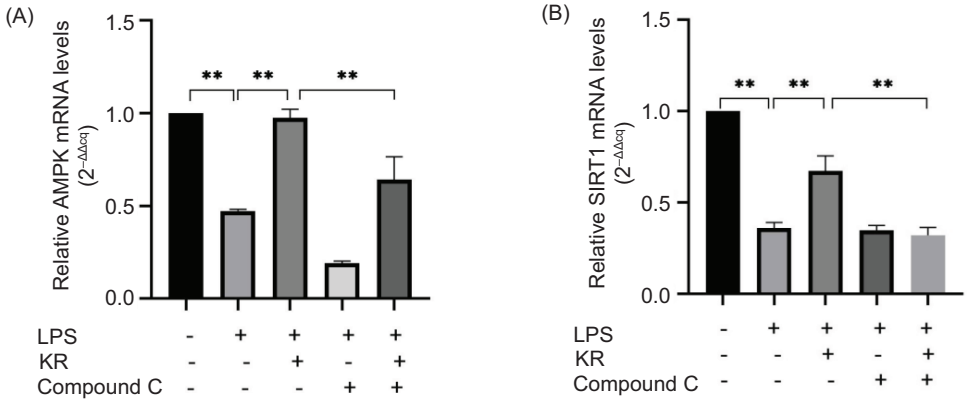

Figure 7. Effects of kaempferol-3-O-rutinoside (KR) and Compound C on the proteins of AMPK/SIRT1 signal pathway. (A) p-AMPK, (B) SIRT1. The values are expressed as mean ± SD (n = 3). **p < 0.01 vs the model group; **p < 0.01 vs the KR group.

its mechanism. KR has a protective effect on the TNF-human umbilical vein endothelial cells (HUVEC) injury model established *in vitro*, and its mechanism is related to its anti-inflammatory and endothelial cell protection (Yu *et al.*, 2021). Previous research has demonstrated that KR could decrease the protein expression levels of TLR4, MyD88, and NF-κB in LPS-induced H9c2 cell injury, indicating that it inhibits inflammatory response through TLR4/MyD88/NF-κB signaling pathway (Hua *et al.*, 2021). Our latest finding has indicated that KR could decrease IL-1β level and inhibited the expression levels of NF-κB, NLRP3, ASC, Caspase-1 p20, GSDMD, and IL-1β, suggesting that the protective effect of KR was related to regulating the NF-κB/NLRP3/Caspase-1 signaling pathway (Hua *et al.*, 2022). Thus, our studies found that KR is closely related to NF-κB. Therefore, it is of great significance to explore whether KR elucidates its myocardial protective effect by regulating the upstream signaling pathway of NF-κB. In this study, molecular docking results showed that KR could bind to AMPK, and its therapeutic effect and correlation with the AMPK/SIRT1 signaling pathway was further studied by *in vitro* experiments. The *in vitro* results have shown that KR could reduce apoptosis rate, reverse the elevated levels of IL-1β, IL-6, and TNF-α, and suppress the expression levels of AMPK and SIRT1, indicating that its anti-inflammatory effect could be achieved by regulating AMPK/SIRT1 signaling pathway.

Conclusion

In this study, the molecular docking prediction combined with *in vitro* validation was performed to study the mechanism of myocardial protection with KR. The protective mechanism of KR on the myocardium was further improved. However, a limitation of this study is that the mechanism of action is still not exhaustive. In the future study, gene silencing and gene overexpression of AMPK or SIRT1 must be added to explore the mechanism of KR.

Acknowledgments

This study was supported by the Open Fund of State Key Laboratory of Tea Plant Biology and Utilization (SKLTOF20210112), and Natural Science Foundation of the AnHui Higher Education Institutions of China (KJ2021A1167).

Author Contributions

Fang Hua and Peng Zhou designed the study and revised the manuscript. Yao-yao Ma, Xiao-ni Zhao, and Lan Zhou carried out the experiments. Sheng-nan Li, Juan Bai, and Ling-li Shi analyzed the data. The manuscript was written by Yao-yao Ma. All authors approved the final version of the paper.

Conflict of Interest

The authors stated that they had no conflict of interest to declare.

Data Availability

The data that supported the findings of this study are available from the corresponding authors upon reasonable request.

Acknowledgment

This study was supported by the Outstanding Youth Scientific Research Project of Anhui Universities (2022AH030158), Natural Science Foundation of the AnHui Higher Education Institutions of China (KJ2021A1167), and the Open Fund of State Key Laboratory of Tea Plant Biology and Utilization (SKLTOF20210112).

References

Bai W.X., Wang C., Wang Y.J., Zheng W.J., Wang W., Wan X.C., et al. 2017. Novel acylated flavonol tetraglycoside with inhibitory effect on lipid accumulation in 3T3-L1 cells from Lu'an GuaPian tea and quantification of flavonoid glycosides in six major processing types of tea. J Agric Food Chem. 65(14): 2999–3005. https://doi.org/10.1021/acs.jafc.7b00239

Chen R., Gao S., Guan H., Zhang X., Gao Y., Su Y., et al. 2022. Naringin protects human nucleus pulposus cells against TNF-α-induced inflammation, oxidative stress, and loss of cellular homeostasis by enhancing autophagic flux via AMPK/SIRT1 activation. Oxid Med Cell Longev. 2022: 7655142. https://doi.org/10.1155/2022/7655142

Chen X., Li X., Zhang W., He J., Xu B., Lei B., et al. 2018. Activation of AMPK inhibits inflammatory response during hypoxia and reoxygenation through modulating JNK-mediated NF-κB pathway. Metabolism. 83: 256–270. https://doi.org/10.1016/j.metabol.2018.03.004

Chen C., Zhou M., Ge Y. and Wang X. 2020. SIRT1 and aging related signaling pathways. Mech Ageing Dev. 187: 111215. https://doi.org/10.1016/j.mad.2020.111215

D'Alessandra Y., Chiesa M., Carena M.C., Beltrami A.P., Rizzo P., Buzzetti M., et al. 2020. Differential role of circulating microRNAs to track progression and pre-symptomatic stage of chronic heart failure: A pilot study. Biomedicines. 8(12): 597. https://doi.org/10.3390/biomedicines8120597

Deng H.J., Zhou C.H., Huang L.T., Wen L.B., Zhou M.L. and Wang C.X. 2021. Activation of silent information regulator 1 exerts a neuroprotective effect after intracerebral hemorrhage by deacetylating NF-κB/p65. J Neurochem. 157(3): 574–585. https://doi.org/10.1111/jnc.15258

Herzig S. and Shaw R.J. 2018. AMPK: guardian of metabolism and mitochondrial homeostasis. Nat Rev Mol Cell Biol. 19(2): 121–135. https://doi.org/10.1038/nrm.2017.95

Hua F., Li J.Y., Zhang M., Zhou P., Wang L., Ling T.J., et al. 2022. Kaempferol-3-O-rutinoside exerts cardioprotective effects through NF-κB/NLRP3/Caspase-1 pathway in ventricular remodeling after acute myocardial infarction. J Food Biochem. 46(10): e14305. https://doi.org/10.1111/jfbc.14305

Hua F., Zhou P., Liu P.P. and Bao G.H. 2021. Rat plasma protein binding of kaempferol-3-O-rutinoside from Lu'an GuaPian tea and its anti-inflammatory mechanism for cardiovascular protection. J Food Biochem. 45(7): e13749. https://doi.org/10.1111/jfbc.13749

Hua F., Zhou P., Wu H.Y., Chu G.X., Xie Z.W. and Bao G.H. 2018. Inhibition of α-glucosidase and α-amylase by flavonoid glycosides from Lu'an GuaPian tea: molecular docking and interaction mechanism. Food Func. 9(8): 4173–4183. https://doi.org/10.1039/C8FO00562A

Hurley D.J., Irnaten M. and O'Brien C. 2021. Metformin and glaucoma-review of anti-fibrotic processes and bioenergetics. Cells. 10(8): 2131. https://doi.org/10.3390/cells10082131

Li Y., Yu X., Wang Y., Zheng X. and Chu Q. 2021. Kaempferol-3-O-rutinoside, a flavone derived from *Tetrastigma hemsleyanum*, suppresses lung adenocarcinoma via the calcium signaling pathway. Food Func. 12(18): 8351–8365. https://doi.org/10.1039/D1FO00581B

Liu Y., Grimm M., Dai W.T., Hou M.C., Xiao Z.X. and Cao Y. 2020. CB-Dock: a web server for cavity detection-guided protein-ligand blind docking. Acta Pharmacol Sin. 41(1): 138–144. https://doi.org/10.1038/s41401-019-0228-6

Schumacher D., Alampour-Rajabi S., Ponomariov V., Curaj A., Wu Z., Staudt M., et al. 2019. Cardiac FGF23: new insights into the role and function of FGF23 after acute myocardial infarction. Cardiovasc Pathol. 40: 47–54. https://doi.org/10.1016/j.carpath.2019.02.001

Sun J.H., Yang H.X., Yao T.T., Li Y., Ruan L., Xu G.R., et al. 2021. Gentianella acuta prevents acute myocardial infarction induced by isoproterenol in rats via inhibition of galectin-3/TLR4/MyD88/NF-κB inflammatory signalling. Inflammopharmacology. 29(1): 205–219. https://doi.org/10.1007/s10787-020-00708-4

Tang T.J., Wang X., Wang L., Chen M., Cheng J., Zuo M.Y., et al. 2022. Liquiritin inhibits H_2O_2-induced oxidative stress injury in H9c2 cells via the AMPK/SIRT1/NF-κB signaling pathway. J Food Biochem. 46(10): e14351. https://doi.org/10.1111/jfbc.14351

Wang Y., Tang C. and Zhang H. 2015. Hepatoprotective effects of kaempferol 3-O-rutinoside and kaempferol 3-O-glucoside from Carthamus tinctorius L. on CCl4-induced oxidative liver injury in mice. J Food Drug Anal. 23: 310–317. https://doi.org/10.1016/j.jfda.2014.10.002

Wang S., Ye L. and Wang L. 2019. Protective mechanism of shenmai on myocardial ischemia-reperfusion through the energy metabolism pathway. Am J Transl Res. 11(7): 4046–4062.

Wang Y., Zhang S., Ni H., Zhang Y., Yan X., Gao Y., et al. 2021. Autophagy is involved in the neuroprotective effect of nicotiflorin. J Ethnopharmacol. 278: 114279. https://doi.org/10.1016/j.jep.2021.114279

Wu K.K. 2021. Control of mesenchymal stromal cell senescence by tryptophan metabolites. Int J Mol Sci. 22(2): 697. https://doi.org/10.3390/ijms22020697

Wu S. and Zou M.H. 2020. AMPK, mitochondrial function, and cardiovascular disease. Int J Mol Sci. 21(14): 4987. https://doi.org/10.3390/ijms21144987

Xiao B., Sanders M.J., Carmena D., Bright N.J., Haire L.F., Underwood E., et al. 2013. Structural basis of AMPK regulation by small molecule activators. Nat Commun. 4: 3017.https://doi.org/10.1038/ncomms4017

Yu S., Guo Q., Jia T., Zhang X., Guo D., Jia Y., et al. 2021. Mechanism of action of nicotiflorin from Tricyrtis maculata in the treatment of acute myocardial infarction: from network pharmacology to experimental pharmacology. Drug Des Devel Ther. 15: 2179–2191. https://doi.org/10.2147/DDDT.S302617

Yuan Q., Zhang X., Wei W., Zhao J., Wu Y., Zhao S., et al. 2022. Lycorine improves peripheral nerve function by promoting Schwann cell autophagy via AMPK pathway activation and MMP9 downregulation in diabetic peripheral neuropathy. Pharmacol Res. 175: 105985. https://doi.org/10.1016/j.phrs.2021.105985

Zhao D., Liu J., Wang M., Zhang X. and Zhou M. 2019. Epidemiology of cardiovascular disease in China: current features and implications. Nat Rev Cardiol. 16(4): 203–212. https://doi.org/10.1038/s41569-018-0119-4

Zhao F., Meng Y., Wang Y., Fan S., Liu Y., Zhang X., et al. 2022. Protective effect of Astragaloside IV on chronic intermittent hypoxia-induced vascular endothelial dysfunction through the calpain-1/SIRT1/AMPK signaling pathway. Front Pharmacol. 13: 920977. https://doi.org/10.3389/fphar.2022.920977

Zhao Y., Sun H., Li K., Shang L., Liang X., Yang H., et al. 2021. Cholinergic elicitation prevents ventricular remodeling via alleviations of myocardial mitochondrial injury linked to inflammation in ischemia-induced chronic heart failure rats. Mediators Inflamm. 2021: 4504431. https://doi.org/10.1155/2021/4504431